E-proceedings of the 36th IAHR World Congress
28 June – 3 July, 2015, The Hague, the Netherlands

FLUID-STRUCTURE-INTERACTION IN PIPE COILS DURING HYDRAULIC TRANSIENTS: NUMERICAL AND EXPERIMENTAL ANALYSIS

DAVID FERRAS[1,2]

[1] *Instituto Superior Técnico, Universidade de Lisboa, Portugal*
david.ferras@ist.utl.pt

[2] *Laboratory of Hydraulic Constructions (LCH), École Polytechnique Fédérale de Lausanne, Switzerland*
david.ferrassegura@epfl.ch

ABSTRACT

The paper presents the analysis of the effect of Fluid-Structure Interaction (FSI) occurring during hydraulic transients in pipe coils, in particular the main developments and findings. The research work comprises the development of mathematical models, their numerical implementation and their validation as compared with experimental evidence. The aim is to model the behavior of toric pipes during hydraulic transients considering both axial stress waves in the pipe-wall and fluid conservation principles. Three FSI mechanisms are taken into account: the shear stress generated between the fluid and the pipe-wall, the axial movement of the pipe induced by its radial deformation and the pipe movement generated by an imbalance of forces at junctions and boundaries. Hence, Poisson, junction and friction coupling are implemented. To describe the coil structural behavior two conceptual models are developed: the first representing the coil as a straight pipe with a moving valve, and the second assuming independent axial deformation in each coil ring. Although the first approach allows an easier generalization of the method, the second model describes more accurately the FSI problem in the pipe coil as experimentally observed. The paper novelty is the identification and description of a FSI phenomenon occurring in coils by means of a four-equation model.

Keywords: hydraulic transients; Fluid-Structure Interaction; friction coupling; junction coupling; Poisson coupling.

1. INTRODUCTION

Among the different damping phenomena affecting water-hammer wave, Fluid-Structure Interaction (FSI) is probably the most dependent to the specific piping system configuration. Generalization is not presently possible, and the calculations have to be treated on a case-by-case basis (Locher *et al.*, 2000; Wiggert & Tijsseling, 2001).

Several methodologies can be approached in FSI problems. The most common is the use of the Finite Element Method (FEM) for the description of the structural motion and the Method of Characteristics (MOC) for the fluid behavior. Despite classic water-hammer problems have been traditionally solved by MOC, only few authors have attempted FSI coupling by means of a unique MOC scheme integrating both, the fluid and the structure, to mention some: Wiggert *et al.* (1987); Tijsseling & Lavooij (1990); Lavooij & Tijsseling (1991). When a solution of this kind is applied, several problems arise such us the coupling between the different pipe vibration modes, space and time discretization due to the different wave celerities within the system, or the correct definition of boundary conditions. To overcome such problems strong assumptions must be added and the model becomes convoluted, making the MOC approach unattractive and not easy to deal with when several vibrating modes are considered.

On the other side, Ferras *et al*. (2014) carried out a stress-strain analysis of toric pipes for inner pressure loads in the context of hydraulic transients. The basic pipe-wall degrees of freedom were analyzed and strain equations were derived for the predominant pipe-wall displacements, which were identified to be in the axial and circumferential directions. As a result, the FSI problem in toric pipes is reduced to these two vibrating modes and bending, shear and torsional pipe movements can be neglected.

The present research aims at the solution of the FSI generated in coil systems during hydraulic transients by means of the implementation of a four-equation model (two-mode model) in a unique MOC scheme. Hence, classic water-hammer equations are combined with Timoshenko beam equations for the axial pipe-wall loading. The different coupling mechanisms (*i.e.* Poisson, friction and junction coupling) are analyzed in order to determine the most suitable assumptions for the description of the coil structural behavior.

2. EXPERIMENTAL DATA COLLECTION

The experimental set up (Figure 1), assembled at Instituto Superior Técnico (Lisbon, Portugal), is composed of a copper pipe of nominal diameter D = 0.02 m, pipe-wall thickness e = 0.001 m and pipe length L = 105 m. The torus radius is R = 0.45 m and 36 rings compose the entire coil. Strain gauges were installed in the middle section of the pipe in order to carry out strain measurements in the axial and in the circumferential directions for different positions of the cross-section. Young's modulus of elasticity and Poisson ratio of the copper material were experimentally determined by measuring

stress-strain states over a straight pipe sample for the experimental range of pressures. The obtained values were Young's modulus of elasticity E = 105 GPa and Poisson ratio n = 0.33.

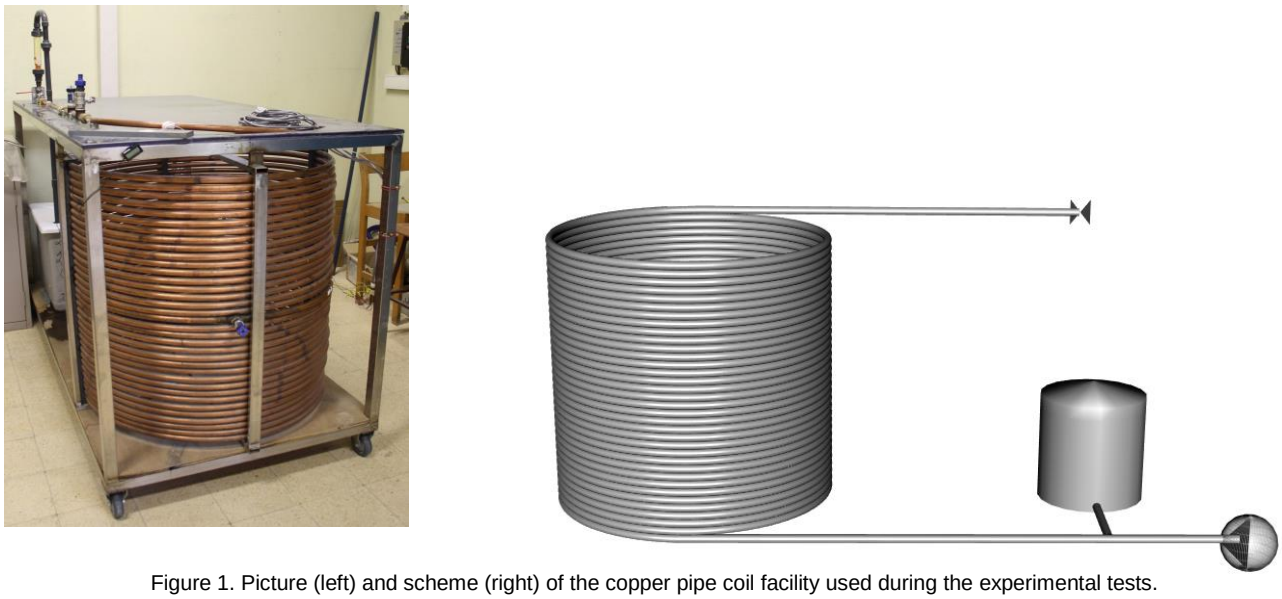

Figure 1. Picture (left) and scheme (right) of the copper pipe coil facility used during the experimental tests.

Several dimensionless parameters indicate when FSI effect might be important (Tijsseling, 1996). Some of these parameters are given in Table 1 for the copper coil experimental facility.

Table 1. Dimensionless parameters for the experimental facility.

ν	a_f/a_s	r/e	ρ_f/ρ_s	E/K	R/r	V/a_f
0.33	0.368	10	8.96	47.95	50	0.00028

Figure 2 depicts measured piezometric head immediately upstream the valve in comparison with the numerical results obtained by the classic water-hammer model for an initial flow rate Q_0 = 400 l/h. The wave amplitude is significantly overestimated by the classic model. The present study tries to correct this discrepancy by assuming that its source is the structural behavior of the coiled pipe system.

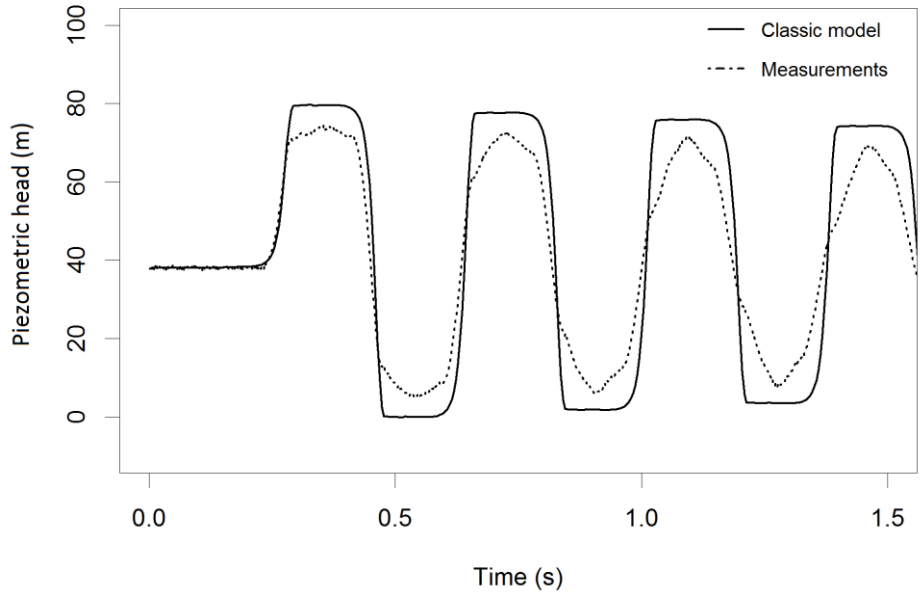

Figure 2. Measured hydraulic head in the downstream boundary in comparison with the classic water-hammer solution for a fast hydraulic transient generated after an initial discharge Q_0 = 400 l/h.

3. MODEL DEVELOPMENT

3.1 Pipe vibration modes

In his development of FSI by integral transforms Skalak (1955) found an infinite number of wave propagation modes. These modes represent the degree of freedom of pipe movement. A classification of one-dimensional FSI models can be made following the basic pipe vibration modes (Tijsseling, 1996):

- One mode: corresponds to the pressure waves calculated only in the fluid (classic water-hammer theory).
- Two modes: axial stress waves in the solid are also described.
- Three modes: includes the radial inertia of the pipe and the fluid.
- Four modes: lateral displacements of the pipe are taken into account
- Seven modes: describes axial motion, flexure and torsional motion of 3D systems.

Based on a previous study (Ferras *et al.*, 2014), radial inertia, flexure and torsion are assumed to be negligible and the FSI in the coil system is described, in the present study, by a four-equation model.

3.2 Four-equation model (two mode)

Skalak (1955) introduced a solution of a 1D four-equation non-dispersive model as an extension of Joukowsky's method. This model was developed by Lavooij & Tijsseling (1991) in all the basic coupling mechanisms (Poisson, junction and friction coupling) solving the following set of equations:

$$\frac{\partial V}{\partial t} + g\frac{\partial H}{\partial x} = -\frac{f}{4r}(V-U)|V-U| \quad [1]$$

$$\frac{\partial V}{\partial x} + \frac{g}{a_f^2}\frac{\partial H}{\partial t} = \frac{2\nu}{E}\frac{\partial S}{\partial t} \quad [2]$$

$$\frac{\partial U}{\partial t} - \frac{1}{\rho_s}\frac{\partial S}{\partial x} = \frac{\rho_f}{\rho_s}\frac{A_f}{A_s}\frac{f}{4r}(V-U)|V-U| \quad [3]$$

$$\frac{\partial U}{\partial x} - \frac{1}{\rho_t a_s^2}\frac{\partial S}{\partial t} = -\rho_f g\frac{r\nu}{eE}\frac{\partial H}{\partial t} \quad [4]$$

Equations 1 and 2 are the fluid momentum and mass conservation equations, whereas Equations 3 and 4 are the homologous pipe second vibration mode conservation equations. *H* is the fluid pressure head, *V* is the fluid axial velocity, *S* is the solid axial stress, *U* is the solid axial velocity, *r* the pipe radius, *e* the pipe-wall thickness, *g* is the gravity acceleration, *f* is the Darcy friction coefficient, *E* the Young's modulus of elasticity of the pipe, ν its Poisson ratio, ρ_f and ρ_s are respectively fluid and solid densities, and a_f and a_s are the wave propagation celerities in the fluid and in the solid, respectively. The wave celerity in the solid corresponds to the axial stress wave being described by

$$a_s = \sqrt{\frac{E}{\rho_s}} \quad [5]$$

Whereas a_f is the fluid wave celerity, which for a non-anchored coil is given by (Ferras *et al.*, 2014):

$$a_f = \sqrt{\left[\left(\frac{1}{K} + (2-\nu)\frac{r}{eE} + 1.33\cdot 10^{-11}\right)\rho_f\right]^{-1}} \quad [6]$$

3.3 Characteristic grid

The set of partial differential Equations 1 to 4 are transformed to ordinary differential equations (compatibility equations) by applying the method of characteristics (MOC) and the resulting equations can be easily integrated over a characteristic grid. This transformation is based on a linear combination of the fundamental equations, mass and momentum conservation, and defining their ratio (λ) as:

$$\frac{1}{\lambda} = \frac{dx}{dt} = \lambda a^2 \quad [7]$$

In this way one independent variable (x) can be cancelled out and the system of equations is converted into ordinary differential equations. Therefore, the grid discretization after this transformation is conditioned to fulfill Courant number Cr = 1.

In a four-equation model, though, two different propagating modes are described, fluid pressure and pipe-wall axial stress waves. Consequently, as the system contains two different wave celerities the condition Cr = 1 cannot be fulfilled using the

same time-space discretization for both phenomena. To overcome this problem two main approaches can be used: wave celerity adjustment in order to keep Courant numbers equal to one by achieving a ratio between celerities of integer numbers and, accordingly, applying leaps in the numerical scheme, as suggested by Schwarz (1978), Wiggert (1986) or Bergant *et al.* (2008); or by applying either temporal or spatial interpolation over the grid, as followed, for example, by Fan (1989), Elansary & Contractor (1990), Bouabdallah & Massouh (1997) or Ghodhbani & Hadj-Taïeb (2013). Tijsseling (2003) proposed a third approach, namely the resolution of an exact solution by means of a mathematical recursion. Methods based on interpolations introduce numerical dispersion and diffusion, while the exact solution is feasible only for verification and validation, since for large simulation times it is computationally expensive. The method applied herein is based on the celerities adjustment.

For instance, when applying Equations 5 and 6 to the copper facility (see properties in Table 1) the celerity values obtained are 1261 m/s for the fluid pressure wave and 3423 m/s for the solid stress wave. Taking into account these values, two different integer ratio numbers were tested: $\frac{a_f^*}{a_s^*} = 1/3$ (being $a_f^* = 1141\, m/s$ for $a_s^* = 3423\, m/s$) and a more accurate $\frac{a_f^*}{a_s^*} = 4/11$ (being $a_f^* = 1245\, m/s$ for $a_s^* = 3423\, m/s$).

The adjustment of wave speeds allows calculations to lie in the grid points. However, inevitably such adjustment leads to a phase error resulting from the adjusted fluid wave celerity. Moreover, in the boundaries and in their vicinities, temporal interpolations are unavoidable. Figure 3 depicts the numerical scheme by applying a ratio $\frac{a_f^*}{a_s^*} = 4/11$.

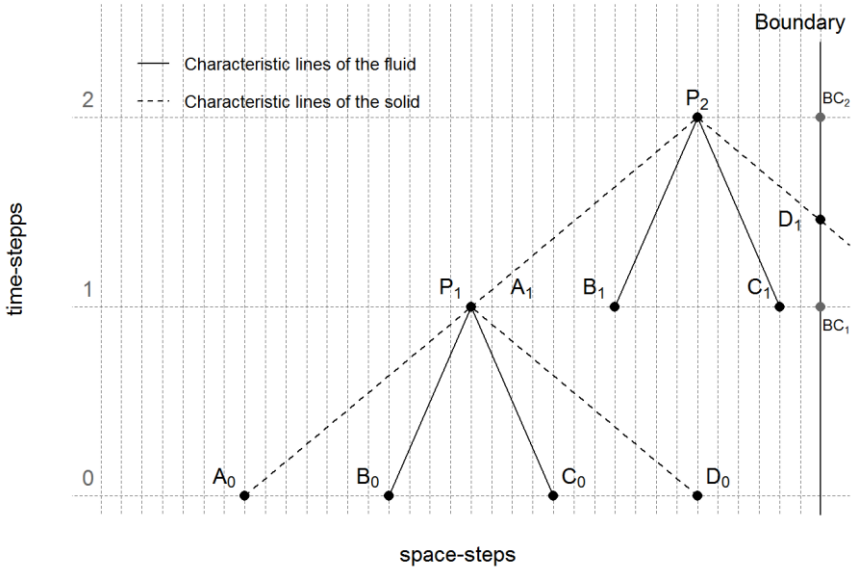

Figure 3. Scheme of the characteristic lines for the wave celerities adjustment $\frac{a_f^*}{a_s^*} = 4/11$.

3.4 Boundary conditions

In a reservoir-pipe-system, the boundary conditions for an infinite reservoir assumption at the upstream-end are

$$H[0,j] = H_{res} \quad [8]$$

$$U[0,j] = 0 \quad [9]$$

While for a fixed valve at the downstream-end are

$$U[l,j] = 0 \quad [10]$$

$$V[l,j] = \tau(t)\sqrt{\Delta H} \quad [11]$$

Where $\tau(t)$ is a function describing the valve maneuver, the coefficients in the squared brackets correspond to space and time coordinates, 0 stands for the upstream boundary and *l* for the downstream boundary, *j* for the time-step, and H_{res} is the pressure head in the reservoir.

For a boundary condition of a moving valve, the balance of forces at this point must take into account the momentum of the valve. Hence, the second law of Newton is applied, describing the rate of change of momentum at the valve as the unbalance of forces over the valve between the fluid pressure and the pipe-wall stress:

$$\rho_f g \Delta H A_f - S[l,j] A_s = m_v \dot{U}[l,j] \quad [12]$$

in which m_v is the mass of the valve, A_f and A_s are, respectively, the fluid and solid cross-sectional areas, and $\dot{U}$ the acceleration of the pipe-wall in the axial direction.

The resulting movement of the pipe generates an axial stress wave that propagates throughout the pipe (junction coupling). Nevertheless, assuming static conditions Ferras *et al.* (2014) showed that the axial stress in a toroidal pipe due to inner pressure is equivalent to the axial stress of a non-anchored straight pipe with closed ends, being $S[l,j] = \frac{Pr}{2e}$, which is indeed the expression of Equation 12 when a massless valve is considered. However, in dynamic conditions, the inertia of the moving element must be taken into account. By rearranging Equation 12 and considering the change of flow rate due to valve closure, the following boundary conditions are obtained:

$$S[l,j] = \frac{\rho_f g \Delta H A_f}{A_s} - \frac{m_v}{A_s} \dot{U}[l,j] \quad [13]$$

$$V[l,j] - U[l,j] = \tau(t)\sqrt{\Delta H} \quad [14]$$

3.5 Model verification

A verification of the basic implementation was carried out by means of the simulation of the well-known Delft Hydraulics FSI benchmark problems from Tijsseling & Lavooij (1990) and Lavooij & Tijsseling (1991). From their set of FSI problems, Problem A is the most suitable to test the developed four-equation model. It consists of a reservoir-pipe-valve system with length L = 20 m, inner radius r = 398.5 mm, pipe-wall thickness e = 8 mm, Young's modulus E = 210 GPa, pipe-wall density ρ_s = 7900 kg/m^3, Poisson ratio ν = 0.30, bulk modulus K_f = 2.1 GPa, fluid density ρ_f = 1000 kg/m^3 and initial flow velocity V_0 = 1 m/s. The valve is closed in one time-step, and both boundary conditions fixed and free moving valve are analyzed.

Corresponding wave speeds are a_f = 1024.7 m/s and a_s = 5280.35 m/s, giving a ratio of a_f/a_s = 0.194. The model has been assessed by a ratio between celerity values of 13/67. Figures 4 and 5 show the model output in comparison with the exact solution of the benchmark problem, as well as the Joukowsky solution, both for a fixed and a moving downstream boundary.

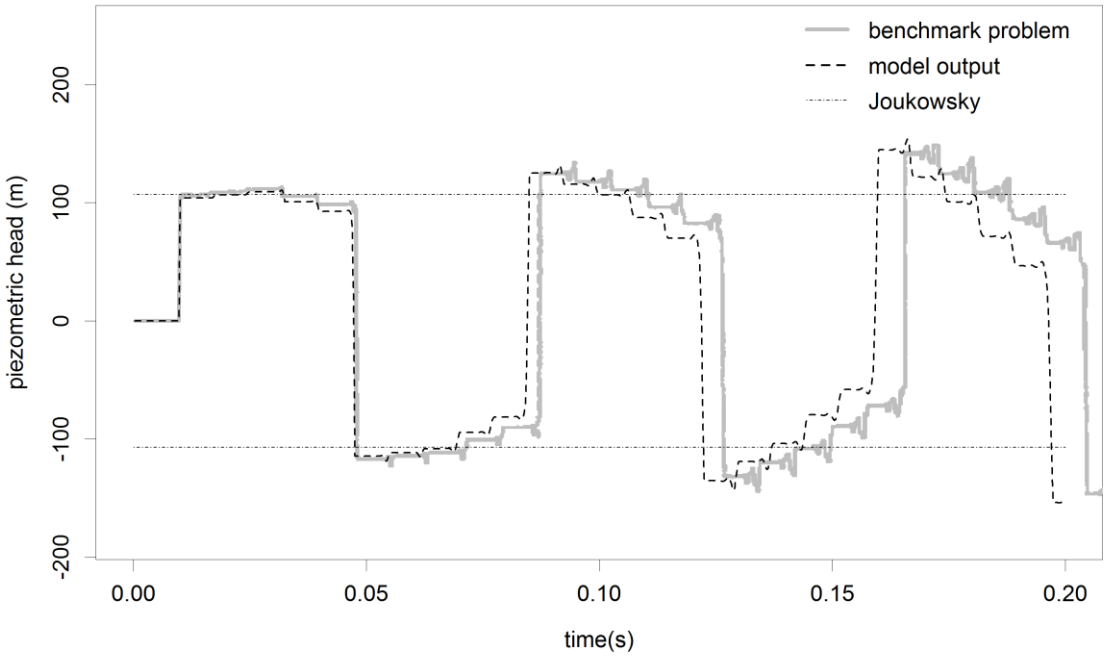

Figure 4. Delft Hydraulics benchmark Problem A for fixed boundaries.

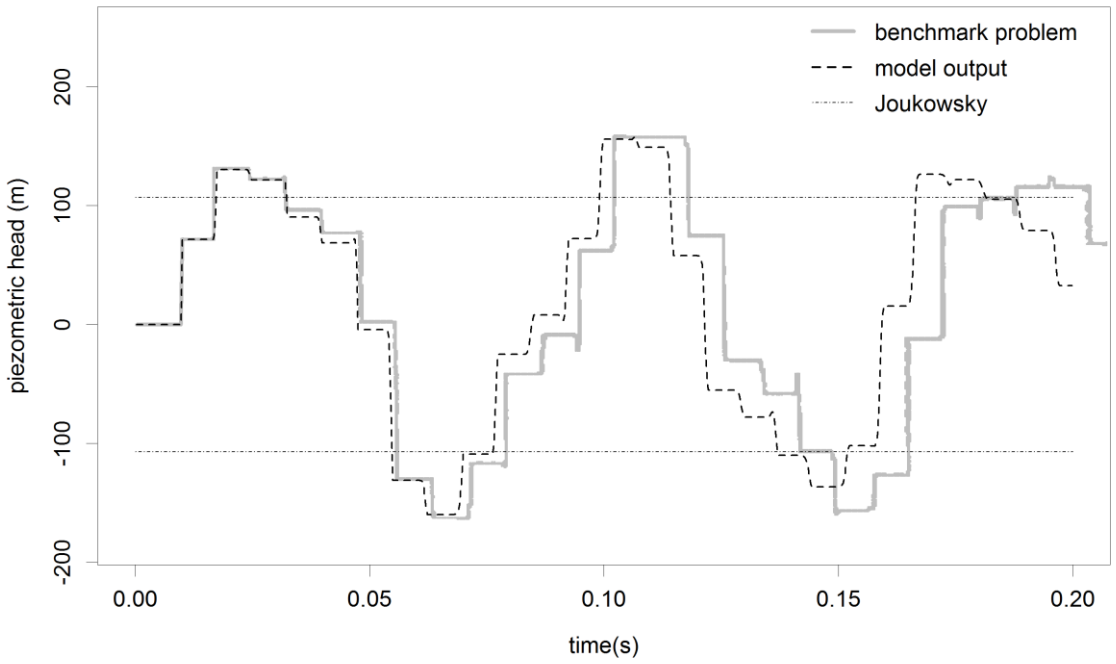

Figure 5. Delft Hydraulics benchmark Problem A for a free moving valve.

Observing Figures 4 and 5 a clear phase shift between the benchmark exact solution and the output of the implemented model can be noticed. The reason of such discrepancy arises from the celerity adjustment. This phase error may be improved by incrementing the accuracy of the ratio between celerity values or by focusing the tuning of the wave speed only in the axial stress wave rather than in the fluid wave, which is the dominant vibrating mode. For the sake of model verification, though, the obtained output achieves the expectations.

4. MODEL APPLICATION

4.1 Modelling assumptions

The coil pipe system, when pressurized, increases its inner volume due to both the axial and the circumferential deformation of the pipe-wall and *vice versa*, for negative pressures, the volume gets reduced. The consequent response of such behavior of the coil over the hydraulic transient wave is a reduction of the wave amplitude ("breathing" effect).

Axial strains of a pipe coil for inner pressure loads in static conditions can be assumed to be equivalent to the ones of a straight pipe with closed ends (Ferras *et al.*, 2014). In the following, two modelling approaches applying the developed four-equation model are analyzed. In Table 2 the basic assumptions for model conceptualization and discretization are depicted.

Table 2. Main modelling assumptions for the simulation of the coil system.

Model parameter	Model-1	Model-2
Vibrating modes	Four-equation model	Two and four-equation model
Geometry	Singular straight pipe	Multi-pipe system
Celerities ratio (a_f/a_s)	4/11	4/11
Modified fluid celerity (a_f^*)	1261 m/s	1261 m/s
Modified solid celerity (a_s^*)	3423 m/s	3423 m/s
Time-step (dt)	0.0025	0.0025
Time-step (dx)	2.83	2.83

4.2 Model-1: straight pipe with moving valve

The implemented four-equation model of Section 3 was used to describe the transient pressures in the coiled copper facility. A reservoir-pipe-valve system with a free moving valve was considered in order to describe the "breathing" effect of the coil due to the axial deformation of the straight pipe. Figure 6 depicts the schematic of the Model-1.

Figure 6. Single straight pipe with a free moving valve at the downstream end.

The model has the following characteristics: pipe length L = 105 m, pipe inner diameter D = 2 cm, pipe-wall thickness e = 1 mm, modulus of elasticity E = 105 GPa, fluid bulk modulus K = 2.19 GPa, fluid density ρ_f = 1000 kg/m^3, solid density ρ_s = 8960 kg/m^3, Poisson ratio ν = 0.33, initial flow velocity V_0 = 0.354 m/s and initial Darcy friction factor f = 0.035 (smooth wall pipe). Figure 7 depicts the model results for a moving massless valve in comparison with the classical water-hammer solution.

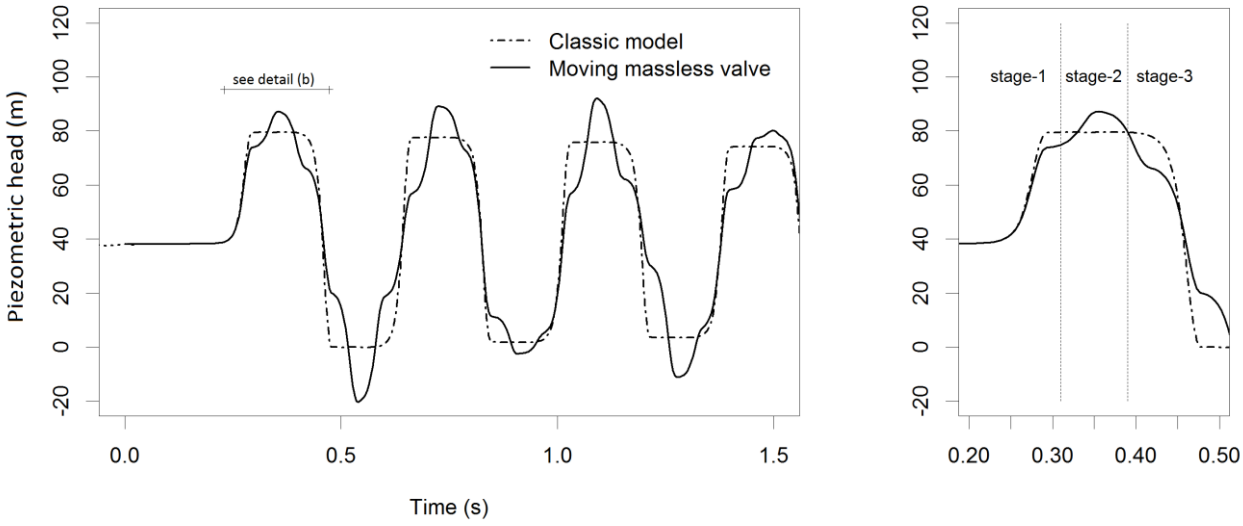

Figure 7. Results of Model-1: a) simulated piezometric head at the pipe downstream end for a free moving massless valve versus results of classic water-hammer solver (left); b) detail of the first peak (right).

Conversely to the classic model output, three stages can be distinguished in the wave pressure peaks in the FSI model output (see Figure 7b): Stage-1 in which the pressure is lower than the classic model; Stage-2 with higher pressure and; finally, Stage-3 with a pressure drop. The first stage is caused by the movement of the valve in the downstream direction after the first pressure surge. Afterwards, as the solid axial stress wave travels approximately 3 times faster than the fluid pressure wave, at around one third of the pressure peak there is an increase of pressure resulting from the negative axial stress which is pulling the pipe upwards, producing this "pumping" effect. Finally, the axial stress wave bounces back pushing again the valve and producing the last pressure drop over the pressure surge.

In order to assess the effect of the moving valve, a sensitivity analysis has been carried out for the valve mass parameter (m_v). A set of 100 simulations from m_v = 0 kg to m_v = 1000 kg was launched.

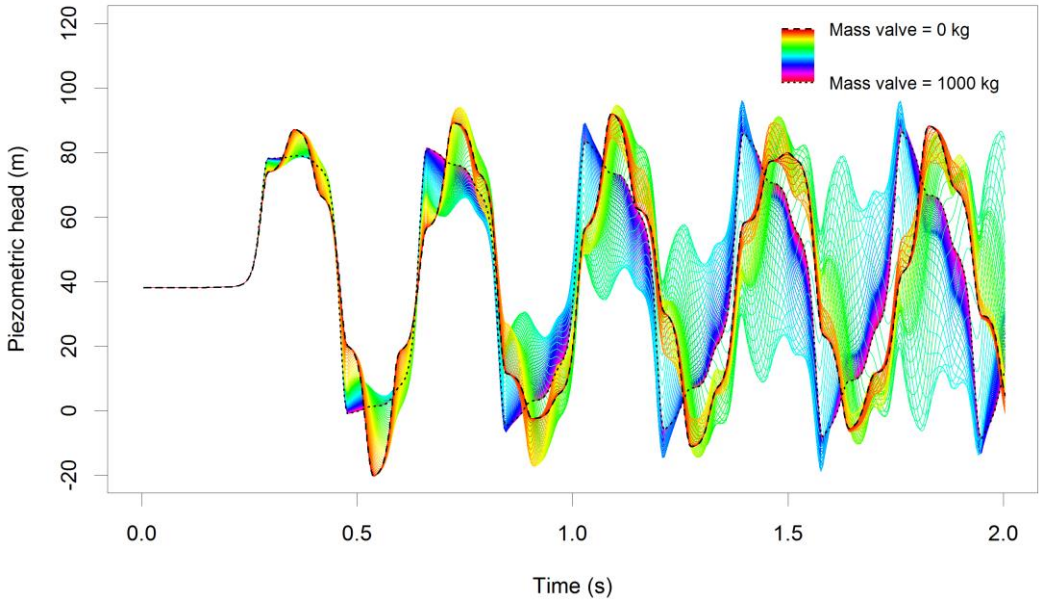

Figure 8. Feasible solution region of Model-1 output for a free moving valve with variable mass. Pressure at the pipe downstream end.

The range of possible solutions of the four-equation model for a free moving valve varying its inertia is shown in Figure 8. The bold dashed line indicates the solution for the minimum valve mass threshold modelled, which is equal to the already presented massless valve solution. The dotted line depicts the output for the maximum valve mass threshold modelled, which is m_v = 1000 kg. As the mass valve increases, results tend to the solution of Poisson coupling with a fixed valve. It is interesting to point out that, due to the dispersion effect of the mass valve, the maximum pressure peak does not occur for an infinite mass valve (fixed valve) nor for a massless valve, but for a solution in-between.

4.3 Model-2: mechanistic model

In order to better describe the observed structural behavior of the pipe coil during the transient pressure wave, a mechanistic model was build using the four-equation FSI model. The approach applies the concept that the rings of the coil vibrate independently from each other according to their inner pressure load in each time-step.

To describe these independent vibrating rings two sorts of models were coupled: 1) a main two equation model representing a straight pipe with a total length of L = 105 m, discretized by 38 nodes and each inner node representing a coil ring; and 2) 36 four-equation sub-models describing the rings behavior. These nested FSI sub-models were built as straight pipes of length equal to the ring perimeter (*i.e.*, 2.83 m) and with closed but free moving ends. The valve in the main pipe is fixed. The model is schematically shown in Figure 9.

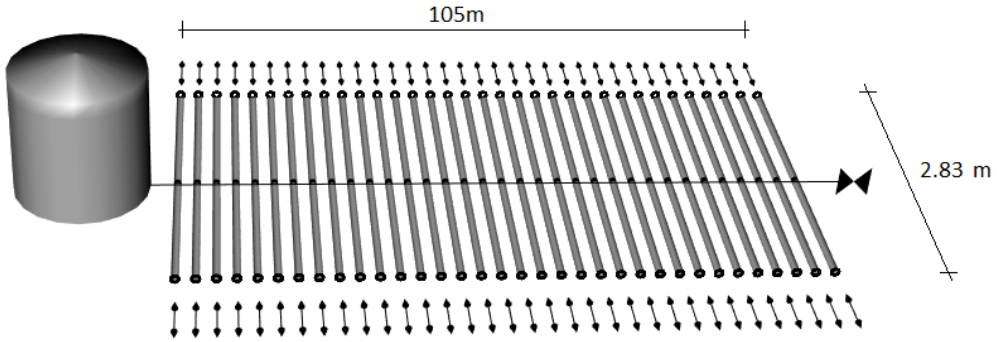

Figure 9. Model-2: independent vibrating rings described by nested FSI sub-models which assume straight pipes with closed free moving ends.

The coupling is carried out by considering the center node of the ring models as the inner node of the main system. In each time-step, the pressure of the rings is equal to the pressure of the entire nested models, consequently the free moving ends stretch or shrink the pipes and describe such ring behavior by giving the feedback from the axial stress equations. This effect produces an increase or decrease of pressure which is transferred to the main pipe. The effect of the moving closed ends can be calibrated by adding inertia to the pipe boundaries (considering the mass of the coil rings).

Finally, velocity must be recomputed in each time-step and node of the main system for the sake of mass and momentum conservation principles.

With the aim of assessing the sensitivity of model output to the rings inertia, a set of 100 simulations was carried out by varying the mass of the rings, from 0 to 1000 kg. Figure 10 shows the output of this set of simulations, where the feasible solution band for the varying mass in the rings is depicted. As it can be observed, the mechanistic model proposed allows the adjustment of the pressure peaks by considering the independent expansion and contraction of the rings according to a certain mass load.

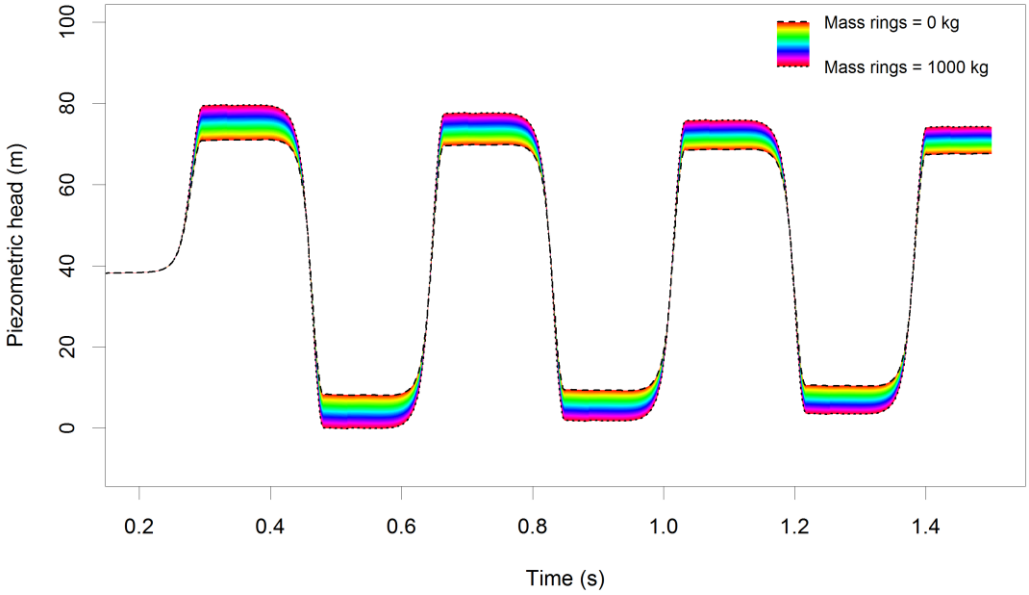

Figure 10. Model-2 output considering a varying mass of the rings in comparison with measured pressure data at the downstream end.

In the mechanistic model an additional sensitivity analysis can be carried out based on the distribution of the mass assigned to the coil rings. The analysis consisted of a set of simulations by enabling the free movement of massless rings throughout the coil except one fixed ring. Each ring was iteratively assessed carrying out a total of 36 simulations. The output allowed the analysis of the effect of the fixed ring over the pressure output. Figure 11 depicts hydraulic head during the first peak for the mentioned set of simulations. A deeper assessment of this sensitivity analysis can be found at (Ferras *et al.*, 2015).

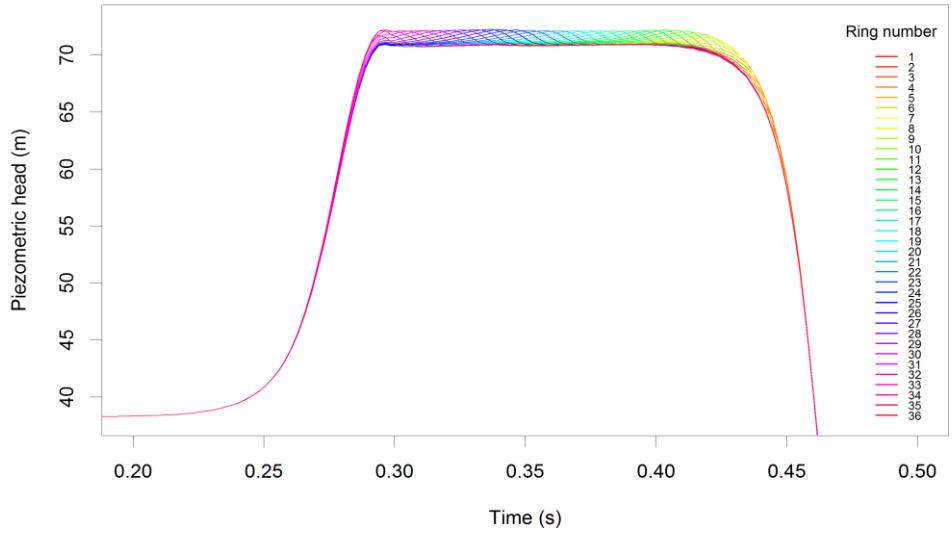

Figure 11. Model-2 output of the first pressure peak for a set of 36 simulations by allowing the free movement of the rings except one. The position of the fixed ring is changed in each simulation ($1 == upstream\ ring\ is\ fixed$; $36 == downstream\ ring\ is\ fixed$).

5. DISCUSSION OF RESULTS

Model-1 simplifies the coiled pipe system to a straight pipe with a moving valve at its downstream end, while Model-2 describes the independent vibrating rings by assuming a mechanistic model. Figures 12 and 13 show the results of the best simulations from both models (with lower MSE at the first pressure peak) at two pipe sections: at the downstream end and at the intermediate section. The best simulation of Model-1 is obtained with a valve mass of 121 kg. The best simulation of Model-2 corresponds to a total mass of the rings of 100.8 kg over the coil.

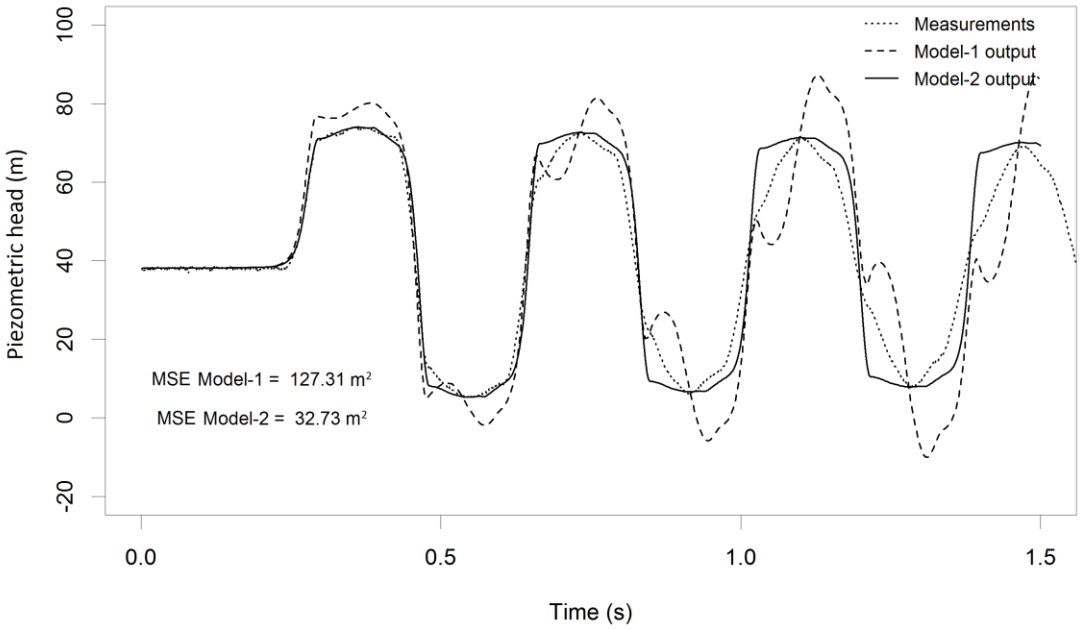

Figure 12. Pressure outputs at the downstream end of the pipe from the best simulations of Model-1 and Model-2 in comparison with measurements. Computed MSE are shown for both models.

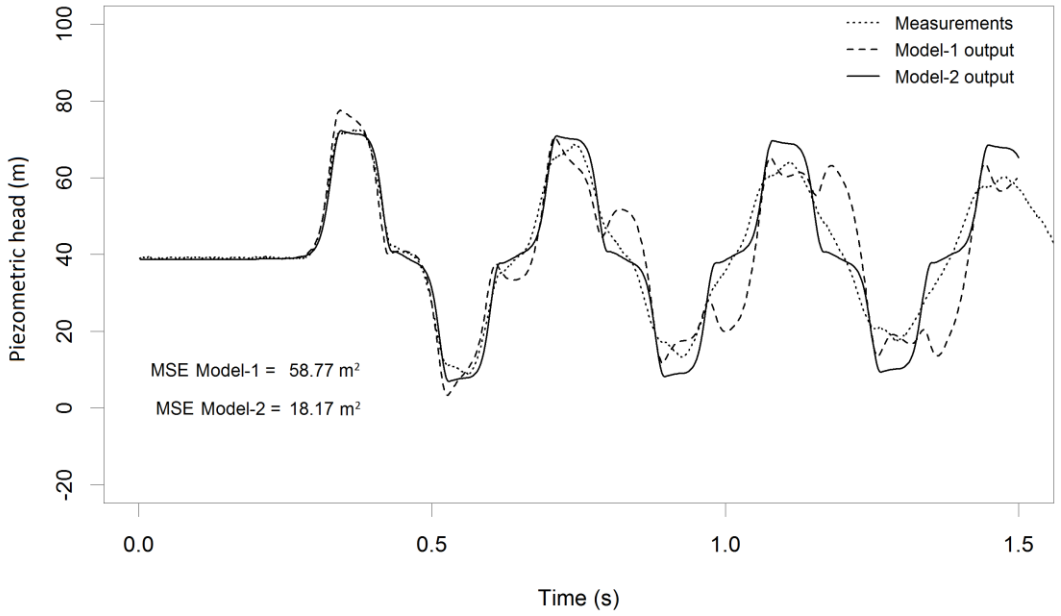

Figure 13. Pressure outputs at the middle section of the pipe from the best simulations of Model-1 and Model-2 in comparison with measurements. Computed MSE are shown for both models.

The previous figures show the pressure output of both models in comparison with measured data: Figure 12 at the pipe downstream end and Figure 13 at the middle section. Although Model-1 enables the description of the pressure variation according to pipe-wall axial deformation, the model does not describe with accuracy the shape of the pressure wave. Consequently, the mean squared error is quite high in comparison to Model-2 for both gauging locations. On the other side, Model-2 presents very good agreement with measured data for the first pressure peak, since the distributed mass of the rings allows an accurate calibration of the pressure wave shape. However, the calibrated wave shape in the first pressure peak does not evolve according to the observed propagation of the transient event. The reason may be that other physical phenomena, relevant during the propagation of the water-hammer wave, have not been taken into account, such as unsteady friction, possible anelastic behavior of the pipe-wall, viscoelasticity of the anchors of the coil rings or friction between the coil structure and its supporting structure. Moreover, other pipe vibrating modes not taken into account in the four-equation model could also affect the coil system, such as shear, bending and torsion of the pipe.

It is important to point out that the main difference between the two models depends on how junction coupling is considered. In Model-1 the junction coupling is focused on the balance of forces over the valve (boundary condition). In Model-2, junction coupling results from the balance of forces in each coil ring (internal conditions). In the experimental coil system, the moving elements are the rings and not the valve, hence Model-2 is more faithful to the real phenomenon. However, the mechanistic model proposed does not solve entirely the FSI problem, as solid variables are only partially solved. Therefore, stress and strains cannot be fully analyzed by means of Model-2. On the other side, Model-1, although less accurate, can be used to analyze both fluid and solid variables. Its intrinsic simplifying assumptions allow the FSI problem to be analyzed by a lighter, but more reliable and robust four-equation model composed of a straight pipe with a moving end.

6. CONCLUSIONS

A mathematical model that describes the Fluid-Structure Interaction occurring in a coil pipe during hydraulic transient events is developed. The method is based on the implementation of a four-equation model, which takes into account the effect of axial stress waves throughout the pipe-wall. The assumption of neglecting shear, flexure and torsional motion of the coil was verified in a previous study of stress-strain analysis (Ferras *et al.*, 2014). To the author's knowledge this is the first time this approach has ever been applied in coiled pipe systems.

In the four-equation model two transient events are coupled, *i.e.* the solid and fluid transient waves in the pipe axial direction. Fluid interacts with its containing structure through three different coupling mechanisms: Poisson, junction and friction coupling. After the implementation of a basic FSI four-equation model and its verification by means of the Delft Hydraulics benchmark problem, two models were developed with the goal to adapt to the coil singularities. The main difference between the two models is how junction coupling is considered. A first attempt was carried out by assuming a single straight pipe with a moving valve at its downstream end (Model-1). A second model (Model-2) was developed by fixing the valve and considering that the moving elements are the coil rings, which vibrate independently according to their inner pressure. The models were calibrated by varying the mass of their moving elements.

In Model-1 the epicenter of axial stress waves due to junction coupling is located in the valve, while in Model-2 it is rather distributed throughout the ring bends. In a static analysis this fact does not make any difference as both models would return equal stresses for equal pressure loads. Though, as shown in the present study, when fluid variables are dynamically interacted with solid variables, the source of the axial stress wave does matter. Moreover, Model-2 enables a distributed mass on the coil rings, allowing a greater capability for calibration. Consequently, Model-2 after calibration is more accurate than Model-1.

Both models confirm the initial hypothesis that the cause of the discrepancy between the experimental measurements and the output from the classic water-hammer model, stated in section 3, stems from the interaction between the fluid and the coil structural behavior. It is shown that this error can be corrected by means of a four-equation model, which covers the coupling of the fluid pressure wave with the solid axial stress wave, hence describing the "breathing" effect of the coil due to the longitudinal movement of the pipe-wall. Model-1 is a good first approximation to tackle the FSI problem. However, the conceptual simplification of reducing the coil to a straight pipe with free moving end does not allow an accurate description of the dynamical behavior of the coil. For this purpose the coil rings movement must be considered. Model-2, using a mechanistic approach, attempts to describe the movement of the coil rings that are not rigidly fixed. After calibration, Model-2 shows a good performance and it allows a more precise description of the dynamics of the FSI occurring in the coil facility. However, the generalization of the second approach is not straightforward and the method must be analyzed on a case by case basis.

ACKNOWLEDGMENTS

This research is supported by the Portuguese Foundation for Science and Technology (Fundação para a Ciência e a Tecnologia) through the project ref. PTDC/ECM/112868/2009 "Friction and mechanical energy dissipation in pressurized transient flows: conceptual and experimental analysis" and the PhD grant ref. SFRH/BD/51932/2012 also issued by FCT under IST-EPFL joint PhD initiative.

REFERENCES

Bergant, A., Tijsseling, A. S., Vítkovsky, J. P., Covas, D. I., Simpson, A. R. & Lambert, M. F. (2008). Parameters affecting water-hammer wave attenuation, shape and timing, part 2: Case studies. Journal of Hydraulic Research 46(3), 382-391.

Bouabdallah, S. & Massouh, F. (1997). Fluid-structure interaction in hydraulic networks. AD-American Society of Mechanical Engineers. Aerospace Division Newsletter.

Chaudhry, H. M. (1987). Applied hydraulic transients. Van Nostrand Reinhold.

Elansary, A. & Contractor, D. (1990). Minimization of stresses and pressure surges. Journal of Pressure Vessel Technology 112(3), 311-316.

Fan, D. (1989). Fluid-structure interactions in internal flows. Ph.D. thesis, Ph. D. Thesis, The University of Dundee, Department of Civil Engineering, Dundee, UK.

Ferras, D., Covas D., and Schleiss A.J. (2014). "Stress–strain analysis of a toric pipe for inner pressure loads." Journal of Fluids and Structures 51: 68-84.

Ferras, D., Covas D., and Schleiss A.J. (2015). "Comparison of conceptual models for Fluid-Structure Interaction in pipe coils during hydraulic transients" Journal of Hydraulic Research (under review).

Ghodhbani, A. & Hadj-Taïeb, E. (2013). Numerical coupled modeling of water hammer in quasi-rigid thin pipes. In: Design and Modeling of Mechanical Systems. Springer, pp. 253-264.

Lavooij, C. & Tijsseling, A. S. (1991). Fluid-structure interaction in liquid-filled piping systems. Journal of fluids and structures 5(5), 573-595.

Schwarz, W. (1978). Druckstossberechnung unter Berücksichtigung der Radial- und Längsverschiebungen der Rohrwandung. Eigenverlag des Inst. für Wasserbau, Univ. Stuttgart.

Skalak, R. (1955). An extension of the theory of water hammer. Tech. rep. Columbia Univ New York Dept of Civil Engineering and Engineering Mechanics.

Tijsseling, A. (1996). Fluid-structure interaction in liquid-filled pipe systems: a review. Journal of Fluids and Structures 10(2), 109-146.

Tijsseling, A. (1997). Poisson-coupling beat in extended waterhammer theory. ASME-PUBLICATIONS-AD 53, 529-532.

Tijsseling, A. (2003). Exact solution of linear hyperbolic four-equation system in axial liquid-pipe vibration. Journal of Fluids and Structures 18(2), 179-196.

Tijsseling, A. & Lavooij, C. (1990). Waterhammer with fluid-structure interaction. Applied Scientific Research 47(3), 273{285.

Wiggert, D. (1986). Coupled transient flow and structural motion in liquid-filled piping systems: a survey. In: Proceedings of the ASME Pressure Vessels and Piping Conference. Chicago, USA.

Wiggert, D. C. & Tijsseling, A. S. (2001). Fluid transients and fluid-structure interaction in flexible liquid-filled piping. Applied Mechanics Reviews 54(5), 455-481.